[논문] 한국태양에너지학회 논문집
Journal of the Korean Solar Energy Society

Vol. 31, No. 5, 2011
ISSN 1598-6411

Study on Air Humidification Control Method for Fuel Cell Vehicles

Agung Bakhtiar* Choi, Kwang-Hwan**

*Graduate School of Dept. of Refrigeration and Air Conditioning Engineering,
**Dept. of Refrigeration and Air Conditioning Engineering, Pukyong National University

연료전지 차량을 위한 공기가습 조절법에 대한 연구

아궁 박티르*, 최광환**

*냉동공조공학과 대학원, 부경대학교,
**냉동공조공학과, 공과대학, 부경대학교(choikh@pknu.ac.kr)

Abstract

연료전지 차량용에 있어서 공기 가습 및 감습의 중요성은 매우 크다. 특히 PEM(Proton Exchange Membrane) 연료전지에서 수분평형은 총괄시스템성능에 큰 영향을 미치는 요소인데, 이에 관한 중요한 연구가 지금까지 광범위하게 수행되고 있다. 또한 차량과 같이 동적부하 연료전지를 활용하는 분야에 있어서, 전류의 흐름은 차량용 파워 부하에 크게 영향을 받는다. 따라서 전기적 흐름이 발생하면, 이에 따라 수분이 발생하게 되는데, 이러한 응축 수분은 예측이 되며, 수관리 시스템에서 이를 중요한 제어 기준으로 활용한다. 그러므로 적절한 제어방법을 선택하면 유입공기의 온도와 습도의 최적값을 얻을 수 있다. 따라서, 본 논문에서는 PEM 연료전지의 수관리를 위하여 수분전달 모델과 유전알고리즘(genetic algorithm)을 사용하는 제어방법에 초점을 두고 있다.

Key words : 연료전지(Fuel cel)l, 수관리(Water management), 가습(Humidification), 유전알고리즘(Genetic algorithm)

Nomenclature

$\dot{m}$: Mass flow rate, [kg·s^{-1}]
c_d : Electro osmotic drag coefficient
ρ : Density, [kg·cm^{-3}]
M_r : Relative molecular mass, [kg·mol^{-1}]
κ : Permeability, [m^2]
s : Liquid saturation level, [-]
ε : Porosity, [-]
μ : Dynamic viscosity, [m^2·s-1]
T : Temperature, [℃]
δ : Thickness, [m]
λ : Latent heat, [kJ·kg-1]
h : Heat transfer coeff, [W·m^{-2}·K^{-1}]

투고일자 : 2011년 9월 9일, 심사일자 : 2011년 9월 9일, 게재확정일자 : 2011년 10월 17일
교신저자 : 최광환(choikh@pknu.ac.kr)

c_{drag} : Air resistance constant, [-]
v : Vehicle velocity, [m·s^{-1}]
c_{rf} : Rolling resistance coefficient, [-]
I : Current density, [A·m^{-2}]
A : Cross section area, [m^2]
F : Faraday constant, [C·mol^{-1}]
ϕ : Humidity ratio, [g·kg^{-1}]
γ : Specific volume, [m^3·kg^{-1}]
V : Volume, [m^3]
Q : Flow rate, [m^3·s^{-1}]
W : Power, [Watt]

Subscript

cap : *capillary*
$evap$: *evaporation*
rct : *reaction*
sat : *saturated*
liq : *liquid*
vap : *vapor*

1. Introduction

Automobile is one of considerable pollution source against the global level, including a significant fraction of the total greenhouse gas emissions [1]. Using fuel cell in automobiles replace its energy source from fossil fuel into renewable and clean energy, furthermore it reduces the pollution from the point of global protection. Among several types of fuel cells, Proton Exchange Membrane (PEM) fuel cell is one of the most promising candidate, especially for automobile applications. It is because there are its high-energy density at low operating temperature, quick start-up and zero emission [2-4].

The electric current of a vehicle fuel cell is depended on the vehicle's power demand. Since the electrical current was consumed, the fuel cell water production was also generated. Therefore, the liquid water can be predicted and used for an important control reference in water management system.

A flooding level can be seen from the accumulated liquid water in a porous medium and it can indicates the level of the liquid water saturation. Hence this present study proposes an inlet air humidification control system of fuel cell for a vehicle to reach the water balance.

2. Modelling

The vehicle power is modeled as the total powers for rolling resistance, air resistance and kinetic given by Eq. (1) [5].

$$W_v = \underset{(roll)}{m\,g\,C_{rf}|v|} + \underset{(airresist)}{\frac{1}{2}\rho_a|v|^3 c_{drag} A} + \underset{(kinetic)}{mv\frac{dv}{dt}} \quad (1)$$

The water liquid saturation level (s) is the flooding or drying indicator and it can be defined as the volume fraction of the total void space of porous medium occupied by the liquid phase. It means that the higher the value of s, the greater the flooding level is, and vice versa..

$$s = \frac{V_{liq}}{V_{tot}} \quad (2)$$

The present liquid water in a cathode catalyst layer (CCL) is a function of the difference between the water addition and the removal. The water addition is obtained from the fuel cell reaction and the humidity of the input air. The water removals means actually the amount of evaporation and

convection. The water addition can be expressed as the total water production from the oxygen reduction reaction (ORR) and the electro osmotic inside the membrane as given in Eq. (3) [6-8]. Based on ASHRAE standard formula calculating the air properties [9], the water addition from the humid input air can be derived from the relationship beween the humidity and the volumetric flow rate as given in Eq. (4).

$$\dot{m}_{rct} = M_r(c_d + 1)\frac{IA}{2F} \tag{3}$$

$$\dot{m}_{air} = \frac{\phi\, Q}{\gamma} \tag{4}$$

$$\dot{m}_{liq} = \dot{m}_{rct} + \dot{m}_{air} - \dot{m}_{sat} \tag{5}$$

The present liquid water is given by Eq. (5) and also the change of the liquid saturation level will be given by Eq. (6). V_p in Fig. 6 is the volume of porous medium occupied by the gas phase that depends on the degree of its porosity. It means that when there is no liquid water addition, the change of s is zero.

$$\triangle s_{rct} = \frac{\dot{m}_{liq}}{\rho V_p} \tag{6}$$

Many studies were already investigated about the characteristics of the steady state water transportation in gas diffusion layer (GDL) of PEM fuel cell [10,11]. In those researches, it was seen that the capillary transport is the dominant factor in the process to remove the water from the flooded GDLs. The mass flow rate transported by capillary process is given by Eq. (7). The liquid saturation change affected by this capillary process is also given by Eq. (8).

$$\dot{m}_{cap} = s^4(1.417 - 4.240s + 3.789s^2) \times \frac{A\sigma\cos(\theta_c)(\varepsilon\kappa)^{0.5}}{M_r \mu \delta_{GDL}} \tag{7}$$

$$\triangle s_{cap} = \frac{\dot{m}_{cap}}{\rho V_p} \tag{8}$$

In general, the evaporation rate can be calculated by Eq. (9) and the liquid saturation change affected by this evaporation process can be given by Eq. (10). Furthermore the final liquid saturation is defined as Eq. (11).

$$\dot{m}_{evap} = \frac{h(4s+2)(V_p)^{2/3}|T_{liq} - T_{air}|}{\lambda} \tag{9}$$

$$\triangle s_{evap} = \frac{\dot{m}_{evap}}{\rho V_p} \tag{10}$$

$$s_x = s_0 + \triangle s_{rct} - \triangle s_{cap} - \triangle s_{evap} \tag{11}$$

3. Control system

The intermittent control system is used to handle the input air properties. The setting of the input air becomes flexible by every designed control interval. The control interval in this study was set already on 50s. Therefore, the control system started by measuring the current density of the fuel cell within first 50s. This measured data was then used as the control reference on the optimization process using genetics

algorithm (GAs). The fitness function used in this GAs was the water transportation model given by Eq. (11). The outcome of this fitness function also means the difference between the predicted liquid water saturation level and the controlled level as given in Eq. (12).

$$s_{fit} = |s_{target} + s_m| \quad (12)$$

This s_{target} is the controlled liquid saturation level and s_m is the liquid saturation level obtained from the model. The fitness value is the absolute difference between the model result and the target. The smallest s_{fit} value is able to be target of the GAs.

4. Simulation methods

In order to evaluate the performance of the alternative control algorithms, it is useful to take a standard usage pattern against which to test them. Since fuel cells are often associated with automotive applications, this study uses the New European Driving Cycle (NEDC) and the standard velocity-to-time map used in the European Union to test car engines for pollutant emissions. The NEDC is representative of both the urban and the extra-urban driving in Europe, but many other countries and authorities have defined their own set of driving cycles, such as the United States' FTP-75 and Japan's JP 10-15. For those reasons, nine driving cycles were used in this simulation [12] as shown in Table 1 and the parameters used in this simulation are shown on Table 2.

Table 1. Driving cycles

Driving cycle	Max Velocity ($m \cdot s^{-1}$)	Time (s)
NYCC	12.3	599
EUDC	33.3	400
JP 10-15MODE	19.4	660
ECE	13.8	195
FTP72	25.3	1369
FTP75	25.3	1874
NEDC	33.3	1180
SC03	24.4	596
US06	35.8	596

Table 2. Simulation parameters

Parameter	Value
Q	0.08 m^3/s
A	0.02 m^2
δ_{GDL}	3.10^{-4}m
N	448
c_d	0.5
κ	1.810^{-18} m^2
μ	$8.55\ 10^{-4}$ $N.s/m^2$
ε	0.6
σ	0.0625 N/m
h	105.28 W/m^2K
λ	2417.44 kJ/kg

5. Results and discussions

The driving cycles are shown as graphically in Fig. 1. The force has positive while being accelerated. Since the speed has always positive, the power demand becomes positive and this power demand should be met by the power generation system. By applying the driving cycle data, the vehicle power can be calculated using Eq. 1 and then presented in Fig. 2. The EUDC, FTP75 and US06 cycles shown in both figures had the highest average power demand.

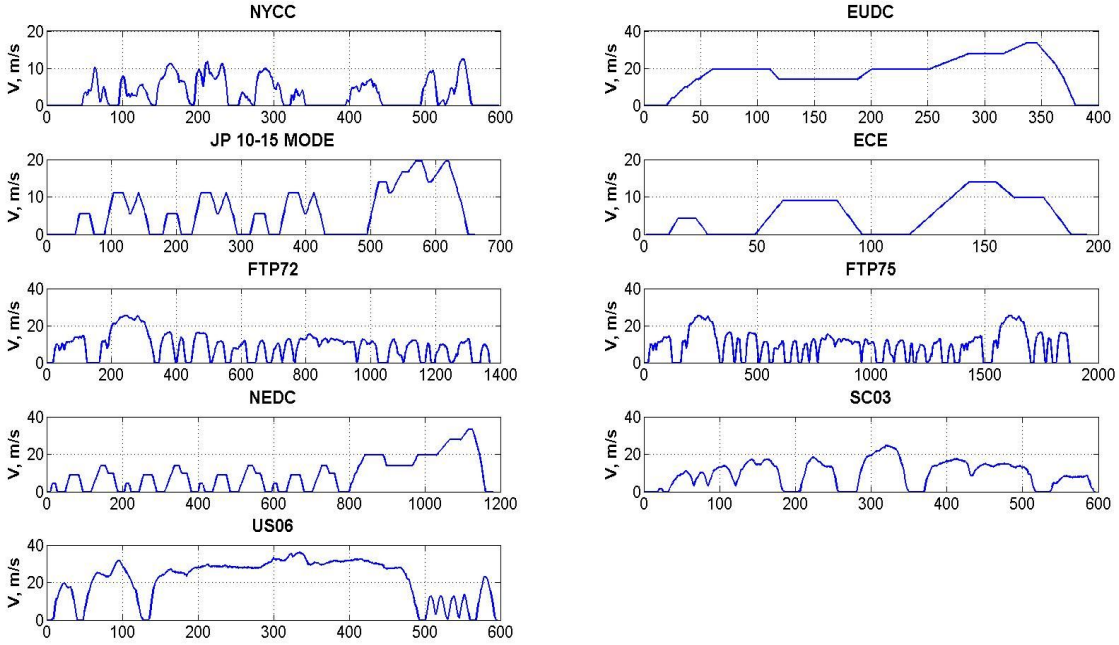

Fig. 1. Different driving cycles in nine standards

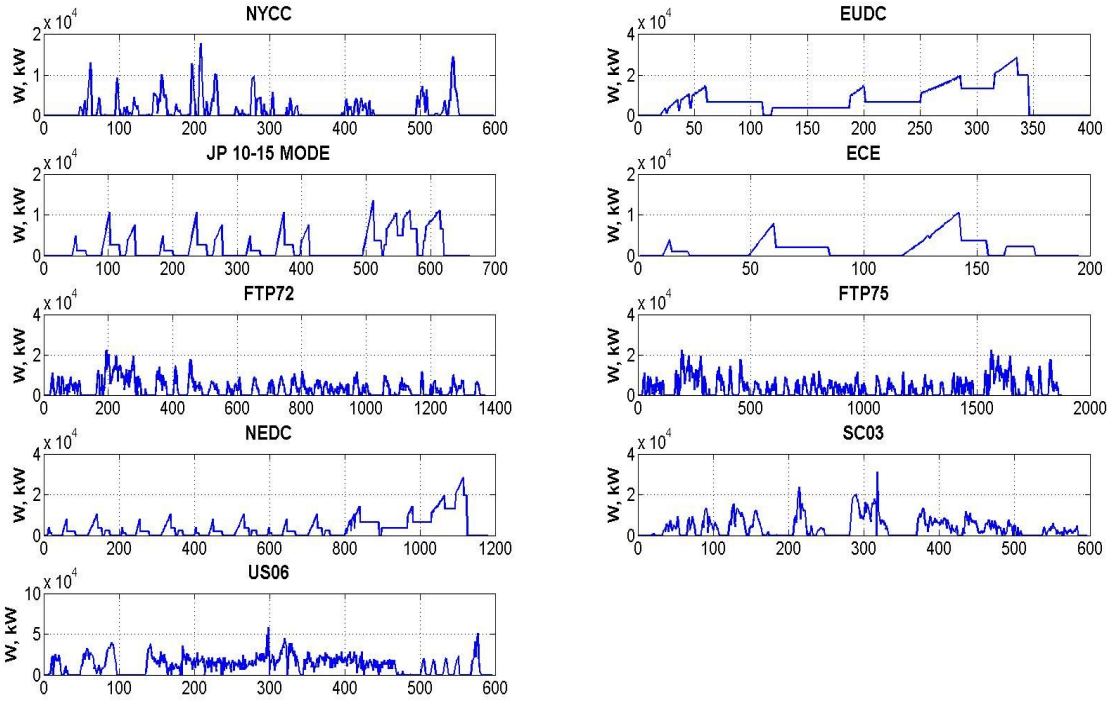

Fig. 2. Power profiles in nine standards

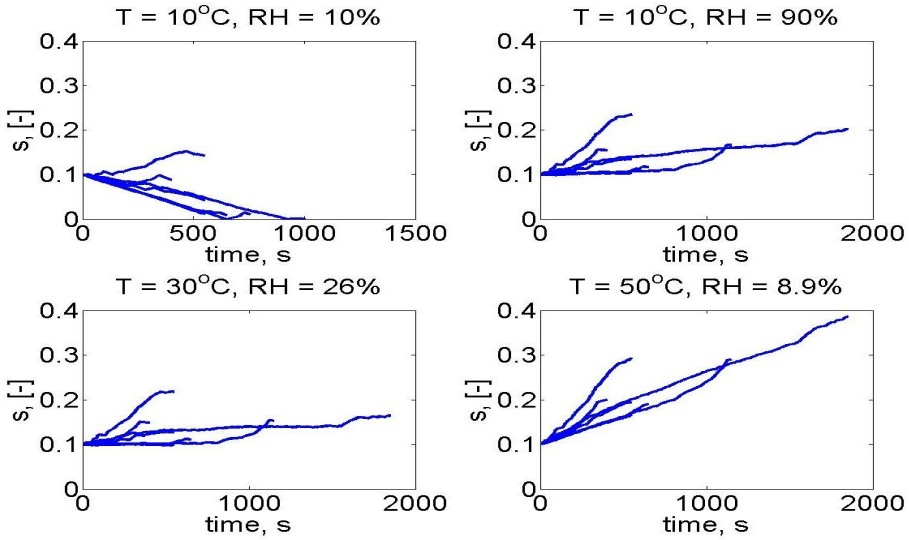

Fig. 3. Simulation result for all driving cycles in varying air condition without control system

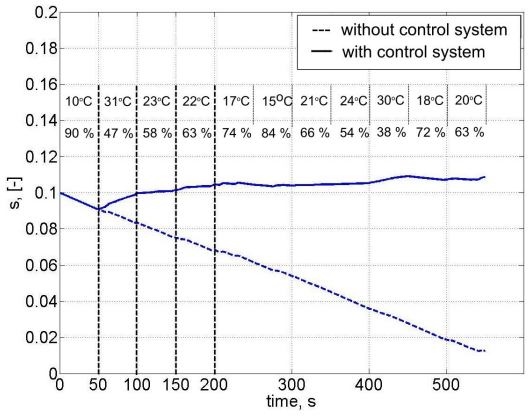

Fig. 4. Simulation results of control system for NYCC (in case of 10°C, 90%)

The simulation results revealed that the different ambient air condition reaches different fuel cell's liquid saturation level profiles as shown in Fig. 3. When the fuel cell is operated under the low temperature and humidity (10°C and 10% RH), the drying tends to happen in almost driving cycles. However, if the humidity increases, some of driving cycles start to get flooding. This is the reason why the inlet air properties should be controlled dynamically to avoid flooding or drying in the process.

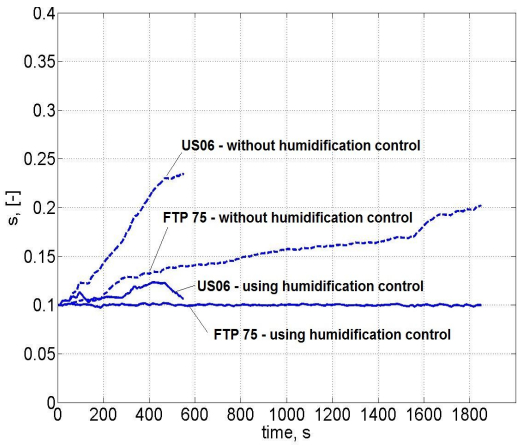

Fig. 5. Simulation result of control system for FTP 75 and US06

The air properties were changed every 50s in order to maintain the liquid saturation level at 0.1. However the results could not be exact 0.1 at the target. This was caused

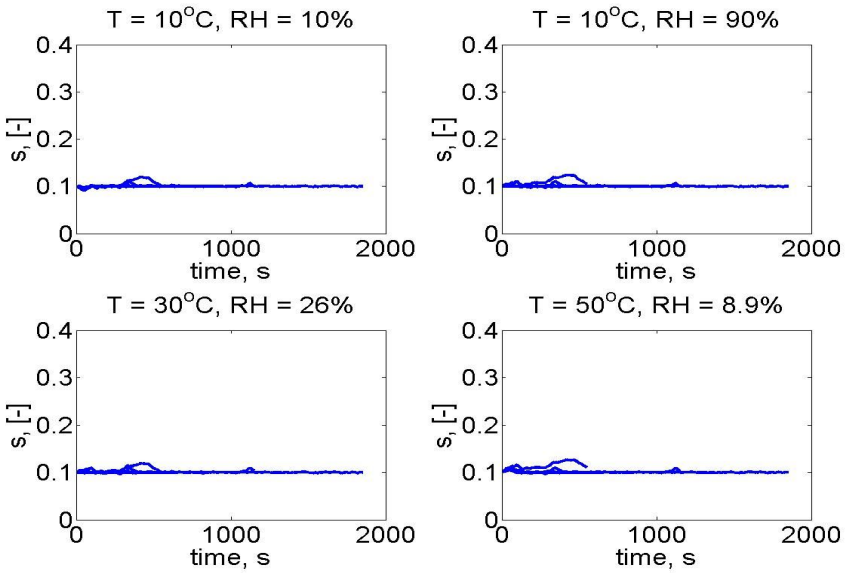

Fig. 6. Simulation result of control system for all driving cycles in varying air condition

by the previous 50s power pattern which could not be perfectly same with the next 50s unknown power pattern.

Fig. 5 shows the control result for the high average power demand such as FTP 75 and US06 profiles. The control results of FTP 75 have shown a little high deviation from the target. This means that controlling inlet air properties was not enough for this condition. Therefore more operating parameter should be also controlled.

The control results for all driving cycles were shown in Fig. 6 against every ambient air condition as shown in Fig. 3. It was clear that the liquid saturation level of every driving cycles were controlled to the target level 0.1. But for high average power demands, the results have shown the greater deviations.

6. Conclusions

In dynamic system, different inlet air condition in cathode side have given different liquid saturation level at cathode. Therefore the dynamic inlet air control system is necessary to be applied to a dynamic fuel cell system. The inlet air condition can not be changed rapidly due to the air conditioning system limitation. Hence, the intermittent control is preferred for simple use. This study presents about simulations of the control system with nine driving cycles to investigate the flooding and drying. The simulation was done with and without air humidification control system under the different ambient air condition. The simulation of the intermittent air humidification control system in several driving cycles has shown a relatively good result. The liquid saturation level was kept as seen constant at 0.1 although there are still small deviations at high average power demands.

Reference

1. A. D. Sagar, Environmental Impact Assessment Review, Vol. 15, Issue 3, pp. 241-274, May 1995
2. K. Jiao, B. Zhou, J. Power Sources, Vol. 169, Issue 2, pp. 296-314, June 2007
3. C. Bao, M. Ouyang, B. Yi, Int. J. Hydrogen Energy. Vol. 31, Issue 13, pp 1879-1896, October 2006
4. Kui Jiao, Li Xianguo, Progress in Energy and Combustion Science, Vol. 37, Issue 3, pp. 221-291, June 2011
5. F. Zenith and S. Skogestad, Journal of Process Control, Vol. 19, Issue 3, pp. 415-432, March 2009
6. Mao L., Wang C. Y., J. Electrochem. Soc. Vol. 154, pp. B139-B146, 2007
7. J.S. Yi, J. Deliang Yang, C. King, AIChE J. Vol. 50, pp 2594, 2004
8. Park Y. H., Jerald A. C. International journal of hydrogen energy, Vol. 33, Issue 24, pp. 7513-7520, December 2008
9. ASHRAE, 2001 ASHRAE Fundamentals Handbook. New York, 2001
10. Pasaogullari U., C. Y. Wang, J. Electrochem. Soc, Vol. 154, pp. A399-A406, 2004
11. S. Ge, C.Y. Wang, J. Electrochem. Soc. Vol. 154. pp. B998-B1005, 2007
12. US Environmental Protection Agency, http://www.epa.gov/nvfel/testing/dynamometer.htm, Accessed July 2011